# Rifaximin prophylaxis causes resistance to the last-resort antibiotic daptomycin

A.M. Turner[1], L. Li[1], I.R. Monk[1], J.Y.H. Lee[1,2], D.J. Ingle[1], S. Duchene[1], N.L. Sherry[1,3,4], T.P. Stinear[1], J.C. Kwong[1,4], C.L. Gorrie[1,3]*, B.P. Howden[1,3,4]*† and G.P. Carter[1]*†

[1]Department of Microbiology & Immunology, The Peter Doherty Institute for Infection and Immunity, The University of Melbourne, Melbourne, VIC, Australia

[2]Department of Infectious Diseases, Monash Health, Clayton, VIC, Australia

[3]Microbiological Diagnostic Unit Public Health Laboratory, Department of Microbiology and Immunology, The University of Melbourne at The Peter Doherty Institute for Infection and Immunity, Melbourne, VIC, Australia

[4]Department of Infectious Diseases, Austin Health, Melbourne, VIC, Australia

*These authors supervised this work equally.

†**Corresponding authors:** glen.carter@unimelb.edu.au, bhowden@unimelb.edu.au

## Abstract

Bacterial pathogens such as vancomycin-resistant *Enterococcus faecium* (VREfm) that are resistant to almost all antibiotics are among the top global threats to human health. Daptomycin is a new last-resort antibiotic for VREfm infections with a novel mode-of-action, but for which resistance has surprisingly and alarmingly been widely reported. The causes of such a rapid emergence of resistance to this novel antibiotic have been unclear. Here we show that the use of rifaximin, an unrelated antibiotic used prophylactically to prevent hepatic encephalopathy in liver disease patients, is causing resistance to this last-resort antibiotic in VREfm. We show that mutations within the bacterial RNA polymerase complex confer cross-resistance to both rifaximin and daptomycin. Furthermore, VREfm with these mutations are

spread globally across at least 5 continents and 20 countries, making this a major yet previously unrecognised mechanism of resistance. Until now, rifaximin has been considered 'low-risk' for development of antibiotic resistance. Our study shows this is not the case and that widespread rifaximin use may be compromising the clinical efficacy of daptomycin, one of the major last-resort interventions for multidrug resistant pathogens. These findings demonstrate that unanticipated antibiotic cross-resistance may potentially undermine global strategies designed to preserve the clinical use of last-resort antibiotics.

## Main

Antimicrobial resistance (AMR) is one of the greatest public health threats that humanity currently faces, with 1.27 million deaths being directly attributable to bacterial AMR in 2019[1]. The magnitude of this threat is therefore similar to that of malaria (558,000 global deaths in 2019)[2], HIV (690,000 deaths in 2019)[3], and diabetes mellitus (1.5 million deaths in 2019)[4]. Infectious caused by multidrug (MDR) and extensively drug resistant (XDR) pathogens are of particular clinical concern since they are associated with frequent treatment failure and high-rates of morbidity and mortality. The preservation of last-resort antibiotics that can be used to treat these formidable pathogens is of critical importance.

*Enterococcus faecium* is one such formidable pathogen. It is a commensal of the human gastrointestinal tract that has emerged as a major nosocomial pathogen[5]. The intrinsic antibiotic resistance of hospital-associated clones coupled with their ability to rapidly acquire additional antibiotic resistance genes makes *E. faecium* infections increasingly difficult to treat[6]. In particular, strains resistant to vancomycin, the first-line antibiotic for invasive infections, have emerged and disseminated globally due to the acquisition of transferable *van*

resistance genes[7]. Consequently, *E. faecium*, which is one of the ESKAPE pathogens (*Enterococcus faecium*, *Staphylococcus aureus*, *Klebsiella pneumoniae*, *Acinetobacter baumannii*, *Pseudomonas aeruginosa*, and *Enterobacter spp*.), has been recognised by the World Health Organization (WHO) as a 'high priority' bacterial pathogen[8].

The lipopeptide daptomycin is a WHO designated 'last-resort' antibiotic that is used 'off-label' to treat severe vancomycin-resistant *E. faecium* (VREfm) infections[9]. The increasing reports of daptomycin-resistant VREfm are of great clinical concern. The specific risk factors for acquiring a daptomycin-resistant VREfm strain are poorly understood, however, patients with a daptomycin-resistant, bloodstream isolate are generally more likely to have been exposed to daptomycin[10,11]. Daptomycin resistance in clinical strains is commonly associated with the presence of specific mutations in the regulatory system LiaRS and cardiolipin synthase Cls[12–14]. However, many daptomycin-resistant VREfm contain wild-type (WT) *liaRS* and *cls* alleles, indicating other unknown molecular pathways are involved[13,15,16].

In Australia, high rates (15%) of daptomycin-resistant VREfm were recently reported[17], but the data were not epidemiologically robust and genetic determinants leading to resistance were not defined. Accordingly, we undertook a combined genomic and phenotypic analysis to investigate the daptomycin resistance mechanisms in VREfm. Here we show that daptomycin resistance can emerge *de novo* in VREfm following exposure to rifaximin, a commonly prescribed antibiotic used prophylactically to prevent hepatic encephalopathy[18] in liver disease patients. Further, we show that rifaximin-mediated daptomycin resistance is linked with the presence of novel mutations (G482D, H486Y, and S491F) within the rifampicin-resistance determining region (RRDR) of RpoB. Importantly, patients given rifaximin were

significantly more likely to harbour daptomycin-resistant VREfm (that also carried RpoB mutations) than patients who did not receive rifaximin. Finally, we show that the identified RpoB mutations arose within the VREfm population soon after rifaximin was first approved for clinical use and have since become globally established, with three independent VREfm lineages currently circulating within at least 20 countries. Our work has therefore uncovered a major new mechanism of daptomycin resistance in VREfm and identified rifaximin, an antibiotic considered to be low-risk for the emergence of bacterial resistance[19], as an important driver of last-resort antibiotic resistance.

## Results

### Daptomycin resistance in Australian VREfm is polygenic and does not correlate with known resistance determinants.

Daptomycin susceptibility testing was performed on VREfm isolated during two unbiased state-wide 'snapshot' studies undertaken for month-long periods in 2015 (n=294) and 2018 (n=423) in Victoria, Australia. The proportion of isolates resistant to daptomycin was 16.6% (n=49) in 2015 and 15.3% (n=65) in 2018. Given the unexpectedly high rate of resistance observed, we expanded the study to include additional VREfm isolated in 2017 (n=108) and 2018 (n=173) as part of the 'Controlling Superbugs' flagship study[20,21], with 28.4% (n=80) of these isolates being resistant to daptomycin. Overall, we observed 189 (18.9%) daptomycin-resistant VREfm isolates, indicating a very high prevalence of daptomycin resistance in Victoria, Australia.

To investigate the relationship between daptomycin-resistant and daptomycin-susceptible VREfm, whole-genome comparisons were made for the 998 study isolates plus two additional

finished VREfm genomes (one daptomycin-susceptible and one daptomycin-resistant). A maximum-likelihood phylogeny was inferred from an alignment of 6,574 core genome single nucleotide polymorphisms (SNPs) (Supplementary Figure 1). *In silico* multi-locus sequence typing identified 36 sequence types (STs) within the 1000 isolates; 30 of these STs included at least one of the 189 daptomycin-resistant VREfm. Daptomycin resistance was interspersed throughout the tree (i.e. mostly polyphyletic), with several distinct clades. The largest clade (ST203) of daptomycin-resistant strains, accounted for 42.3% of resistant isolates (n=80 of 189) and consisted of a single clone predominant during our sampling timeframe (2015 to 2018), suggestive of an expanding daptomycin-resistant lineage. The other predominant STs (ST80, ST796, ST1421, and ST1424) consisted of several groups of resistant isolates that did not cluster based on tree structure. The presence of daptomycin-resistant isolates in distinct genetic backgrounds suggested daptomycin resistance has arisen independently within this VREfm population on multiple occasions.

Given the high prevalence of daptomycin resistance in Australian VREfm isolates, we sought to determine the genetic determinants leading to resistance. Only seven daptomycin-resistant isolates (3.7%) contained the dual LiaR W73C and LiaS T120A mutations. This finding is of note since current literature suggests these mutations are the most important mechanism of daptomycin resistance in VREfm[9,12,22]. In addition, no daptomycin-resistant isolates contained the H215R or R218Q mutations in Cls or the Q75K mutation in the septum site determining protein (DivIVA), which have all previously been linked with daptomycin resistance in VREfm[23]. The mechanism of daptomycin resistance in the majority (n=182) of our resistant study isolates was therefore left largely unexplained by previously characterised mutations.

**The S491F mutation in RpoB is a novel mediator of daptomycin resistance in VREfm.**

To identify the mutations associated with daptomycin resistance in our study isolates, we performed a genome-wide association study (GWAS) approach on the collection of 1,000 VREfm isolates with known daptomycin MIC (Figure 1A). To account for the clonal population structure of the collection, we first removed non-homoplastic variants from the list of core genome mutations to reduce the data set to variants that were acquired at least twice across the phylogeny. We then applied a linear mixed model using a kinship matrix as a random effect. After correcting for multiple testing, the analysis identified 142 mutations (in 73 genes) significantly ($P < 1x10^{-10}$) associated with daptomycin resistance (as a binary variable with a breakpoint of 8 mg $L^{-1}$). The top five most significant mutations were (i) I274S in an uncharacterised ABC efflux protein ($P = 7.44x10^{-15}$), (ii) G71S in an uncharacterised permease protein ($P = 7.77x10^{-14}$), (iii) V288L in a mannitol dehydrogenase protein ($P = 6.08x10^{-12}$), (iv) S491F in RpoB, which is the RNA polymerase ß subunit ($P=1.57x10^{-13}$), and (v) T634K in RpoC, which is the RNA polymerase ß' subunit ($P=4.40x10^{-11}$).

Deletion of the genes encoding the ABC efflux protein, permease protein, or mannitol dehydrogenase protein had no impact on daptomycin susceptibility in a clinical daptomycin-susceptible strain of VREfm from the ST796 genetic background. Similarly, introduction of the T634K mutation within RpoC did not lead to increased levels of daptomycin resistance. However, introduction of the S491F substitution within RpoB, resulted in a 4-fold increase in daptomycin MIC, from 2 mg $L^{-1}$ to 8 mg $L^{-1}$, and a daptomycin-resistant phenotype. Since mutations within *rpoB* have previously been associated with daptomycin resistance in *Staphylococcus aureus*[24,25], we focused further experimental investigations on the RpoB S491F mutation.

145

146 Based on amino acid alignment, the S491F mutation is located within the predicted RRDR of
147 *E. faecium* RpoB, which spans amino acids 467 to 493 (inclusive). The majority of study isolates
148 (n=829, 82.9%) contained a WT RRDR; however, 169 (16.9%) VREfm contained at least one
149 mutation within this region (Figure 1B), with the S491F mutation being the most common
150 (n=105). This was followed by H486Y (n=16), G482D (n=12), G482V (n=10), Q473L (n=6),
151 H486R (n=5), and other uncommon (n=3) mutations.

152

153 **Different mutations within the RRDR of RpoB result in daptomycin resistance in VREfm.**
154 Given the association of the S491F mutation in RpoB with daptomycin resistance, we
155 hypothesised that other mutations within RpoB may also alter daptomycin susceptibility
156 (Figure 1B). In keeping with this hypothesis, we observed a putative correlation between
157 strains carrying individual G482D (n=12) and H486Y (n=16) mutations in RpoB and daptomycin
158 resistance, with 10 daptomycin-resistant isolates containing G482D (83.3% resistant) and 13
159 containing H486Y (81.3% resistant). Clinical isolates containing the G482D, H486Y, or S491F
160 mutations were interspersed throughout the phylogenetic tree and identified in distinct STs,
161 highly suggestive of multiple independent acquisitions (Figure 1C). Ongoing expansion was
162 also observed for one dominant, daptomycin-resistant clone (ST203) containing the S491F
163 mutation throughout the isolate collection period (2015-2018).

164

165 The G482D and H486Y mutations were also located within the predicted RRDR region,
166 suggesting a potential correlation between rifamycin and daptomycin resistance. Therefore,
167 rifampicin susceptibility testing (with rifampicin being a marker of rifamycin resistance[26]) was
168 performed on all clinical VREfm containing a RpoB mutation within the predicted RRDR

(n=169). A randomly selected collection (n=169) of isolates containing a WT RpoB RRDR were used as a control group in this analysis. Mutations located within the predicted RRDR correlated with high-level rifampicin resistance (median MIC 256 mg $L^{-1}$), while control isolates containing the WT region displayed a median MIC of 8 mg $L^{-1}$ (Supplementary Figure 2). The correlation between rifampicin and daptomycin resistance in clinical strains containing the G482D, H486Y, and S491F mutations, suggested a novel link between rifamycin and daptomycin resistance in VREfm.

To confirm the G482D and H486Y mutations in RpoB also led to rifamycin and daptomycin resistance we constructed isogenic mutants carrying these mutations in the same rifamycin-susceptible, daptomycin-susceptible, clinical strain of VREfm (ST796), used to make the S491F RpoB isogenic mutant above. Introduction of the G482D, H486Y, or S491F RpoB mutations resulted in a 7-fold decrease in rifampicin susceptibility compared to the WT strain, leading to high-level rifampicin resistance (>512 mg $L^{-1}$) (Figure 1D). To confirm the changes in rifampicin susceptibility were due to the introduction of each specific mutation and not unknown secondary mutations, we reverted each RpoB mutation to WT by restoration of the chromosomal allele. Complementation to the WT *rpoB* allele in each of the G482D, H486Y, or S491F mutants resulted in reversion of rifampicin MIC to the WT level (8 mg $L^{-1}$), indicating the RpoB mutations were responsible for the heightened levels of rifampicin resistance observed (Figure 1D). To then determine if the G482D and H486Y mutations could also cause daptomycin resistance, daptomycin susceptibility testing was performed. Similar to the S491F isogenic strain, introduction of the G482D or H486Y mutation resulted in a 4-fold increase in daptomycin MIC, from 2 mg $L^{-1}$ to 8 mg $L^{-1}$, and a daptomycin-resistant phenotype (Figure 1E). Complementation with the WT *rpoB* allele onto the chromosome resulted in reversion of

193 daptomycin MIC to the WT level, indicating the G482D, H486Y, and S491F RpoB mutations
194 resulted in cross-resistance to rifamycins and daptomycin in VREfm.
195
196 Given the reported importance of *liaRS* mutations in daptomycin-resistant VREfm, we also
197 introduced the well-characterised LiaR W73C and LiaS T120A mutations into the same clinical
198 strain of VREfm (Figure 1D). No difference in rifampicin MIC was observed after introduction
199 of the *liaRS* mutations, compared to the WT strain, indicating the cross-resistance observed
200 with the G482D, H486Y, and S491F mutations is unique to these RpoB substitutions. However,
201 compared to the WT, introduction of the *liaRS* mutations decreased daptomycin susceptibility
202 2-fold, with a reversion to the WT daptomycin MIC after complementation with the WT *liaRS*
203 alleles. The introduction of the *liaRS* mutations had less of an impact on daptomycin
204 susceptibility than the G482D, H486Y, and S491F RpoB mutations and did not result in a
205 daptomycin-resistant phenotype (MIC $\geq$8 mg $L^{-1}$). When considered in conjunction with the
206 genomic epidemiology data associated with this study, where *liaRS* mutations were less
207 common than the *rpoB* mutations in daptomycin-resistant VREfm (n=7 versus n=141,
208 respectively), our data suggests that mutations within RpoB might represent a previously
209 uncharacterised, yet important mechanism of daptomycin resistance in VREfm.
210
211 **The G482D, H486Y and S491F RpoB mutations are common in international VREfm strains.**
212 To determine if the *rpoB* mutations associated with daptomycin resistance observed in
213 Australian VREfm were representative of other VREfm isolates globally, we performed a large-
214 scale analysis using publicly available VREfm sequence data from healthcare-associated
215 strains (n=4,476; n=3,476 international and n=1,000 Australian) (Figure 2A). Of the isolates
216 analysed, 630 (14.3%) carried an amino acid substitution in the RRDR of RpoB, occurring at 16

positions (Figure 2B). The S491F mutation was the most common, being present in 461 isolates, and accounting for 77.9% of the RpoB mutations observed. Isolates carrying this mutation originated from 20 countries, and *in silico* MLST showed the mutations were spread across 21 different STs, with ST203 (44.7%), ST80 (30.2%), and ST117 (11.5%) accounting for the majority (86.4%) of isolates carrying this substitution. Importantly, five VREfm harbouring the S491F mutation also contained the *cfr(B)* (n=4) or *poxtA* (n=1) genes that confer resistance to linezolid, suggesting near pan-resistant strains of VREfm have already emerged.

The H486Y mutation was the second most common, and was identified in 73 isolates, equivalent to 11.6% of strains with mutations within the RRDR of RpoB. These isolates were collected from 10 countries and *in silico* MLST identified 22 STs, with the most common being ST203 (23.2%), ST796 (21.9%), and ST80 (20.5%). The G482D mutation was the third most common, being identified in 43 isolates, and accounting for 6.8% of strains carrying RpoB mutations. It was present in nine distinct STs, although mostly commonly in ST796 (65.1%) and ST1421 (11.6%), and was identified in isolates from seven countries. Collectively, these data indicated the G482D, H486Y, and S491F mutations, which confer cross-resistance to rifamycins and daptomycin, are not restricted to Australian VREfm but are globally prevalent in healthcare-associated VREfm strains.

To determine whether the identified RpoB mutations were enriched within healthcare-associated VREfm (established as clade A1), we interrogated publicly available genomic sequences of VREfm from clade A2 (n=98), known for being animal-associated[27]. In keeping with previous findings, the maximum-likelihood tree clustered isolates into two main clades: one healthcare-associated and one associated with VREfm from animals. No mutations were

identified in the RpoB RRDR region of strains isolated from animals, with our analyses showing that RRDR RpoB mutations were significantly ($P$<0.001; Fisher's exact test) associated with healthcare-associated VREfm. This suggests the identified RpoB mutations are primarily enriched within the healthcare setting (Supplementary Figure 3).

**Phylodynamics indicate the S491F RpoB mutation emerged within the VREfm population following the clinical approval of rifaximin.**

Given the predominance of the S491F mutation in globally distributed VREfm populations, we used evolutionary phylodynamic analyses to understand its emergence. Within our Australian isolates, we observed the expansion of a dominant ST203 clone from 2015 to 2018 that carried the S491F mutation (Figure 1C). Since this clone comprised VREfm carrying the *vanA* resistance cluster or operon, we sequenced all "historical" *vanA*-VREfm from our public health laboratory (n=229), which consisted of every *vanA*-VREfm isolate collected from 2003 to 2014, to increase temporal signal. We then contextualised all Australian isolates (n=1,229) with the international (n=3,389) VREfm in a maximum-likelihood phylogeny inferred from an alignment of 9,277 SNPs and used clustering with core-genome MLST (cgMLST) to identify three clusters containing the RpoB S491F mutation (Figure 3A). The same ST203 clone (Cluster 1) formed the largest cluster (n=219 taxa), consisting of isolates from Australia and United Kingdom. Cluster 2 (n=85 taxa) consisted of ST80 and ST78 isolates from Australia, Europe, South America, the United Kingdom, and the United States of America while Cluster 3 (n=68 taxa) consisted of ST80 isolates from Australia, Europe, and the United Kingdom.

To model the evolutionary trajectories of these three VREfm clusters, we used core-genome SNP diversity and year of isolation (Figure 3B). Bayesian phylodynamic analyses were

conducted using the core-genome SNP alignments for each cluster/lineage with a discrete trait model and constant coalescent tree prior. We assessed for temporal signal within each cluster using a root-to-tip regression (Supplementary Figure 4). The substitution rate (the number of expected substitutions per site per year) was consistent with other estimates for healthcare-associated VREfm, otherwise referred to as clade A1[27–30]. The median substitution rate was similar for Cluster 1 and Cluster 2, at $9.7 \times 10^{-7}$ [95% highest posterior density (HPD) $6.88 \times 10^{-7} – 1.24 \times 10^{-6}$] and $1.25 \times 10^{-6}$ (95% HPD $7.68 \times 10^{-7} – 1.74 \times 10^{-6}$) respectively, but slightly faster for Cluster 3 at $3.86 \times 10^{-6}$ (95% HPD $2.23 \times 10^{-6} – 5.69 \times 10^{-6}$). The year of emergence for the most recent common ancestor (MRCA) was estimated for each cluster to indicate when the RpoB S491F mutation was first acquired. The MRCAs for the clusters were similar, with 2006 (HPD 1993 – 2012) for Cluster 1, 2000 (HPD 1989 – 2008) for Cluster 2, and 2004 (HPD 2001 – 2010) for Cluster 3, suggesting the lineages emerged at similar times (Figure 3C).

Given the association of the S491F mutation in RpoB and rifamycin resistance, we hypothesised rifamycin use might be driving the emergence of this mutation. The most commonly used rifamycin antibiotics in clinical practice are rifampicin and rifaximin. Since rifampicin was approved for clinical use by the United States Federal Drug Administration (FDA) in 1971, several decades before the estimated emergence of the MRCAs, it is unlikely to have played a major role in the emergence of the S491F mutation within this VREfm population. However, the MRCA for all three clusters is predicted to have emerged around the same time as the first clinical introduction of rifaximin, in 2004. The acquisition of the same mutation in three genetically distinct lineages at a similar time, provides support for our hypothesis that rifamycin use might be driving selection of the S491F mutation within VREfm. Further, the structure of the three maximum clade credibility (MCC) trees (Figure 3B)

289 suggested the lineages have expanded over time, which may be correlated with the approval
290 and subsequent widespread, international use of rifaximin for the prevention of hepatic
291 encephalopathy since 2010 (Figure 3B).
292
293 The S491F mutation in Cluster 1 and Cluster 2 was found to be stably maintained within each
294 lineage after its acquisition, with few high probability events of reversion to the WT *rpoB*
295 allele, indicative of maintenance after emergence (Supplementary Figure 5A-B). For Cluster
296 3, the RpoB S491F mutation emerged a single time, with high (~0.95) posterior probability of
297 a single acquisition within the cluster and subsequent maintenance (Supplementary Figure
298 5C). There was also an equal posterior probability of either a second acquisition within the
299 cluster or loss of the RpoB S491F mutation within Cluster 3. Overall, the Markov jumps for all
300 three clusters suggests that the S491F mutation emerged and was then subsequently
301 maintained within these globally prevalent lineages. Taken together these data show the
302 S491F mutation has emerged within the VREfm population on several occasions since the
303 early 2000s, with the predicted dates of emergence being closely correlated with the clinical
304 introduction of rifaximin.
305
306 **Rifaximin drives the emergence of daptomycin-resistant VREfm in a murine model of**
307 **gastrointestinal colonisation.**
308 Rifaximin is a non-absorbable oral agent with direct antimicrobial activity in the
309 gastrointestinal tract. It is predominately used to prevent recurrent hepatic encephalopathy
310 in patients with liver cirrhosis[18,31]. Importantly, this patient cohort is high-risk for VREfm
311 colonisation within the gastrointestinal tract[32]. Since the Bayesian phylodynamic analyses
312 highlighted a putative correlation between the S491F RpoB mutation in VREfm and use of

313 rifaximin, we hypothesised rifaximin use may be driving the emergence of this mutation and
314 therefore, daptomycin-resistant VREfm within the gastrointestinal tract of patients receiving
315 this antibiotic. To test this hypothesis, mice were colonised with a clinical, daptomycin-
316 sensitive (MIC 2 mg $L^{-1}$) VREfm strain (Aus0233) containing a WT *rpoB* gene before being
317 administered a human-equivalent dose of rifaximin, rifampicin, daptomycin, or vehicle (Figure
318 4A and Supplementary Figure 6). Rifampicin was chosen as a comparison since it is also a
319 commonly used rifamycin in clinical practice. After 7 days of rifamycin treatment, we
320 observed rifamycin-resistant VREfm in significantly more mice receiving rifaximin (90% of
321 mice) or rifampicin (80% of mice) than in mice that received daptomycin (0% of mice) ($P <$
322 0.0001 and $P < 0.0001$; unpaired *t*-test) or vehicle (0% of mice) ($P < 0.0001$ and $P < 0.0001$;
323 unpaired *t*-test) (Figure 4B).
324
325 For each mouse, we then determined the percentage of individual VREfm isolates that were
326 rifamycin-resistant or daptomycin-resistant. There were significantly more rifamycin-
327 resistant VREfm isolated from mice receiving rifaximin or rifampicin than mice receiving the
328 vehicle control ($P < 0.001$ and $P < 0.01$; unpaired *t*-test) or daptomycin ($P < 0.001$ and $P < 0.01$;
329 unpaired *t*-test) (Figure 4D). Similarly, there was significantly more daptomycin-resistant
330 VREfm in mice receiving rifaximin or rifampicin than vehicle control ($P < 0.05$ and $P < 0.05$;
331 unpaired *t*-test) or daptomycin ($P < 0.05$ and $P < 0.05$; unpaired *t*-test) (Figure 4E). We
332 estimated that daptomycin-resistant VREfm accounted for between 0-41% of the
333 gastrointestinal VREfm population in mice given rifaximin and 0-36% in mice given rifampicin,
334 demonstrating conclusively that rifamycin administration can drive the emergence of VREfm
335 with cross-resistance to rifamycins and daptomycin. Notably, no daptomycin-resistant VREfm
336 were isolated from mice receiving daptomycin, in agreement with prior research[33].

337

338 To identify which mutations were present in the rifamycin-resistant VREfm isolates collected
339 from mice administrated either rifaximin or rifampicin, we randomly selected 150 isolates
340 from each antibiotic group (rifaximin or rifampicin, n=300 total) to undergo WGS, consisting
341 of 100 rifamycin-resistant isolates collected following the last day of treatment and 50 isolates
342 from before rifaximin or rifampicin administration. No mutations in RpoB were identified in
343 any VREfm isolate collected prior to rifaximin or rifampicin exposure. However, following the
344 administration of either rifaximin or rifampicin, VREfm carrying mutations within RpoB were
345 commonly identified. The S491F mutation was most abundant (n=53 and 63, respectively),
346 with all isolates carrying this mutation being daptomycin-resistant (Figure 4F). The H486Y
347 mutation was also commonly identified, albeit less so than S491F, (n=12 and 28, respectively),
348 with all isolates again being daptomycin-resistant. The G482D mutation was the third most
349 commonly identified RpoB mutation (n=15 and 6, respectively), with 13 isolates carrying this
350 mutation being daptomycin-resistant. Note that 2 isolates containing the G482D mutation in
351 the rifampicin treated mice were daptomycin-sensitive, likely due to other confounding
352 mutations within the genome. Other RpoB mutations in addition to S491F, H486Y, and G482D
353 were also identified. These included V135F, L471V, E473L, and H486A, however all VREfm
354 isolates carrying these mutations were daptomycin-sensitive. Importantly, the proportions of
355 each RpoB mutation observed in VREfm collected from the gastrointestinal tract of mice
356 administered either rifaximin or rifampicin, correlated closely the proportions of each
357 mutation observed in our collection of human clinical VREfm isolates, with the S491F
358 mutation most commonly identified, followed by H486Y, and then G482D, suggesting a
359 similar selective pressure (i.e. rifamycin use) found in our mouse experiments might be driving
360 the emergence of similar RpoB mutations within human clinical isolates. Taken together,

these data demonstrate that exposure to rifaximin can drive the emergence of daptomycin resistance in colonising strains of VREfm, through the enrichment of isolates carrying select mutations in RpoB.

**VREfm collected from patients receiving rifaximin are more likely to be daptomycin-resistant than VREfm collected from patients that did not receive rifaximin.**

To further test our hypothesis that rifaximin use might be driving the emergence of daptomycin resistance in VREfm, we performed a case-control analysis of clinical VREfm isolates collected from a retrospective cohort of patients from a single tertiary healthcare centre in Melbourne, Australia over 4 years. The VREfm isolates were stratified according to whether the patient had received rifaximin within 1 month of VREfm isolate collection or not. A total of 50 VREfm strains were identified as being from patients receiving rifaximin. As a control group, we randomly selected 50 VREfm that had been collected from patients that had not received rifaximin. The majority (88%) of these VREfm were screening samples. All isolates were collected over the same time frame and from the same institution.

A maximum-likelihood phylogeny was inferred from an alignment of 12,430 core-genome SNPs (Figure 5A). The VREfm isolates in the rifaximin and control groups were dispersed throughout the tree, with 5 different STs (ST78, ST80, ST203, ST796, ST1421, and ST1424) from rifaximin patients and 6 different STs (ST17, ST78, ST80, ST203, ST796, ST1421, and ST1424) from the control patients. There were 28 VREfm from the rifaximin group that contained a mutation within the RRDR of RpoB, with 17 containing the S491F mutation, 5 G482D, 4 H486Y, 1 E473L, and 1 G482V mutation. All isolates containing the S491F, H486Y, and G482D mutations were resistant to daptomycin, while isolates with the E473L and G482V

385 mutations were daptomycin-susceptible. The control group had 2 isolates with RRDR RpoB
386 mutations, with 1 susceptible isolate containing a D476Y and 1 daptomycin-resistant isolate
387 containing the S491F substitution.
388
389 Rifaximin exposure in patients was significantly correlated with the isolation of a rifamycin-
390 resistant ($P$ = 0.00007, OR = 60.0, 95% CI = 8.8 – 2562.1; Fisher's Exact Test) and daptomycin-
391 resistant VREfm strain ($P$ = 0.0006, OR = 25.0, 95% CI = 5.5 – 235.3; Fisher's exact test) (Figure
392 5B and C). These data indicated that patients receiving rifaximin are significantly more likely
393 to carry rifamycin-resistant and daptomycin-resistant strains of VREfm than patients who did
394 not receive rifaximin, suggesting rifaximin use might be an important driver in the *de novo*
395 emergence and spread of daptomycin-resistant VREfm.
396
397 **Discussion**
398 In this study we have shown that specific mutations within the RRDR of RpoB represent a new,
399 major mechanism of daptomycin resistance in VREfm. Our analyses demonstrate these
400 mutations are globally distributed within the VREfm population and are as prevalent as other
401 well-characterised mutations within LiaRS and Cls, which have been previously associated
402 with daptomycin resistance in VREfm and assumed to be the dominant mechanisms[22,34,35].
403 Given the similar prevalence, as well as the finding that isogenic mutants carrying the G482D,
404 H486Y or S491F RpoB mutations display a greater level of daptomycin resistance than isogenic
405 strains carrying mutations in LiaRS, the RpoB mutations discovered here add to the list of
406 clinically relevant mutations involved in the emergence of daptomycin-resistant VREfm.
407

Our data suggest the S491F substitution is the dominant RRDR RpoB mutation in VREfm and is present in at least three phylogenetically distinct lineages currently circulating within healthcare systems globally, including in Australia, the United Kingdom, the United States of America, and across Europe. The extent of their dissemination is likely to be underestimated in regions with limited representation in our analyses, such as in Asia, Africa, and South America. It is of clinical concern these lineages have successfully spread over geographic scales and persisted for at least 15 years, since it suggests these globally prevalent lineages might eventually compromise the therapeutic value of daptomycin for treating VREfm infections. The Bayesian analyses provide support the S491F mutation emerged after the first introduction of rifaximin for clinical use, for treatment of travellers' diarrhea, with each of the MCC trees suggestive of subsequent population expansion. In 2010, rifaximin was shown to be efficacious for the prevention of recurrent hepatic encephalopathy in patients with chronic liver disease[18] resulting in a marked increase in its clinical use. As this patient cohort is predisposed to gastrointestinal VREfm colonisation, we hypothesise that the use of rifaximin in this cohort has driven the population expansion of the S491F mutation in VREfm over subsequent years. Further, our data suggests rifampicin is not a significant driver of these RpoB mutations since therapeutic use of rifampicin has occurred since the 1970s and the emergence of VREfm containing these mutations is much more recent. However, appropriately controlled clinical cohort studies will be needed to test these hypotheses.

VREfm isolates carrying the G428D, H486Y and S491F RpoB mutations were resistant to rifamycin antimicrobials, in addition to daptomycin. Mutations within the RRDR of RpoB have been associated with rifamycin resistance in numerous bacterial species[26], with exposure to rifamycins being a well-documented driver in the emergence of rifamycin-resistant clones in

*Staphylococcus*[36–38]. In keeping with this observation, our data suggests the clinical use of rifaximin may be responsible for selecting VREfm isolates harbouring mutations within the RRDR of RpoB and therefore, indirectly driving the emergence of daptomycin-resistant VREfm. Three lines of evidence support our hypothesis: (i) Bayesian phylodynamic analyses show the emergence of phylogenetically distinct VREfm lineages carrying the S491F is temporally linked with the clinical approval of rifaximin in the early 2000s, (ii) animal experiments demonstrated the administration of rifaximin to mice colonised with VREfm led to the emergence of VREfm strains within the gastrointestinal tract that carried mutations within RRDR of RpoB and were resistant to rifamycins and daptomycin, and (iii) an analysis of clinical VREfm isolated from humans showed patients receiving rifaximin were significantly more likely to carry VREfm strains harbouring mutations within the RRDR of RpoB that were resistant to both rifamycins and daptomycin, compared to patients that did not receive rifaximin. It is therefore plausible that rifaximin exposure in this patient cohort might be an important factor in the increasing rates of daptomycin-resistant VREfm that are currently being reported[17,39], through the *de novo* emergence of the RpoB mutations and/or ongoing transmission of resistant strains carrying these mutations. Appropriately controlled clinical cohort studies are needed to dissect this hypothesis. Importantly, given the high rates of daptomycin resistance observed, our results suggest daptomycin should not be used for empiric therapy of invasive VREfm infections in patients who are receiving rifaximin.

Of note is our observation that rifaximin exposure in mice led to the emergence of strains carrying similar RRDR RpoB mutations to those observed in human clinical isolates and the relative abundance of these mutations within isolates collected from the gastrointestinal tract of mice exposed to rifaximin closely resembled the relative abundance of these mutations in

our collection of human VREfm, with S491F, G482D and H486Y being the most abundant mutations in both cases. These observations are suggestive of similar selective pressures, such as rifaximin exposure, being at play in both the controlled mouse experiments of our study and in the human population.

Overall, this research highlights the potentially serious collateral damage that can arise following the introduction of new clinical antibiotic regimens. While the emergence of within-family antibiotic resistance resulting from prophylactic antibiotic use has been described previously[40,41], there are relatively few studies[37] suggesting that prophylactic antibiotics, such as rifaximin, can lead to cross-resistance between unrelated and last-resort antibiotics, as shown here. Careful consideration should therefore be given to the potential impact of prophylactic antibiotics on antimicrobial stewardship practices. Current thinking[42] recommends withholding the use of last-resort antibiotics to limit the emergence and spread of resistance. However, our findings suggest this is not always the case, since gastrointestinal rifaximin exposure can lead to the emergence of daptomycin-resistant VREfm in the absence of daptomycin. Appropriate surveillance for patients colonised in the gastrointestinal tract with nosocomial pathogens and receiving antibiotic treatment for secondary or unrelated conditions is therefore of critical importance in limiting the emergence and spread of new and increasingly antibiotic-resistant clones within the hospital environment.

In conclusion, we have identified a new, globally important mechanism of last-resort antibiotic resistance in VREfm and show that prophylactic rifaximin use is a likely driver of this resistance. These findings demonstrate the ease with which new antibiotic treatment regiments can drive the emergence of novel multidrug resistant pathogens and highlight the

480 negative impact that unanticipated antibiotic cross-resistance can have on antibiotic
481 stewardship efforts designed to preserve the use of last-resort antibiotics. We advocate for
482 the judicious use of all antibiotics.
483

## Methods

### Media and reagents

*E. faecium* was routinely cultured at 37°C in brain heart infusion (BHI) broth (Becton Dickson) or BHI agar (BHIA), BHI solidified with 1.5% agar (Becto Dickson). For electroporation, *E. faecium* was cultured in BHI supplemented with 3% glycine and 200 mM sucrose (pH 7.0). *Escherichia coli* was cultured in Luria broth (LB). Broth microdilution (BMD) MICs were performed in cation-adjusted Mueller Hinton with TES broth (CAMHBT) broth (Thermo Fisher). A concentration of 10 mg $L^{-1}$ chloramphenicol (Sigma Aldrich) was used for plasmid selection in *E. faecium* and *E. coli*. The following antibiotics were used at variable concentrations for susceptibility testing: rifampicin (Sigma Aldrich), rifaximin (Sigma Aldrich), and daptomycin (Cubicin).

Oligonucleotides were purchased from Integrated DNA Technologies and are listed in Supplementary Table 1. Plasmids were purified with Monarch Plasmid Miniprep Kit (NEB). PCR products and gel extractions were purified using Monarch DNA Gel Extraction Kit (NEB). Genomic DNA was purified using the Monarch Genomic DNA Purification Kit (NEB). Phusion and Phire DNA polymerase was purchased from New England Biolabs.

### Bacterial isolates

Bacterial strains used in this study are listed in Supplementary Table 2. Australian bacterial strains were collected across three data projects in the Microbiological Diagnostic Unit Public Health Laboratory (MDU PHL). Two unbiased cross-sectional surveys of VREfm were conducted between 10 November and 9 December 2015 (n=331)[43] and between 1 November and 30 November 2018 (n=323) in the State of Victoria (referred to as the 2015 and 2018 Snapshot). During this period, all VREfm-positive isolates (including screening and clinical samples) collected by laboratories across the state were sent to the MDU PHL. In addition,

this project included *vanA*-VREfm collected from the "Controlling Superbugs" study[20], a 15-month (April-June 2017 and October 2017-2018) prospective study including eight hospital sites across four hospital networks, resulting in 346 VREfm isolates (308 patients) sent for WGS at MDU PHL. The VREfm were isolated from patient samples (including screening and clinical samples) routinely collected from hospital inpatients. For the 'historical *vanA*-VREfm,' every *vanA* isolate collected within MDU PHL was included. This resulted in an additional 225 isolates, sampled between 2008 and 2014.

For publicly available isolates, our aim was to capture the diversity of *E. faecium* circulating globally by including isolates that formed part of several key studies involving hospital-associated VREfm (as of January 2021). To be included, isolates needed to have short-read data available, with geographic location (by country), year of collection, and source (human or animal). Reads were only included if they had a sequencing depth of >50x. To capture the diversity of VREfm circulating in the United States, isolates from human sources were downloaded from the PathoSystems Resource Integration Center[44]. All isolates were confirmed to be *E. faecium* with the Kraken2 database (v.2.1.2)[45]. The final number of international isolates compromised those from Africa (n=8), Asia (n=25), Europe (n=2941), North America (n=424), and South America (n=78) (Supplementary Table 2).

**Antibiotic susceptibility testing**

Daptomycin susceptibility testing was performed using the BMD MIC method as according to CLSI guidelines. In a 96-well plate, a two-fold dilution series (from 32 to 0.5 mg $L^{-1}$) of daptomycin was made in 100 μL volumes of CAMHBT, additionally supplemented with 50 mg $L^{-1}$ $Ca^{2+}$. An inoculum of 100 μL *E. faecium* broth culture adjusted to 1 x $10^6$ CFU $mL^{-1}$ in CAMHBT was then added to each well. After 24 hours incubation, the MIC was defined as the lowest antimicrobial concentration that inhibited visible growth. All assays were performed

in biological triplicate, with the median MIC reported. In accordance with recent guidelines[46], isolates with a daptomycin MIC $\geq$ 8 mg $L^{-1}$ were considered to be daptomycin-resistant. A daptomycin-sensitive strain (AUS0085)[47] and a daptomycin-resistant strain (DMG1700661)[17] were used as a control.

Rifampicin susceptibility testing was performed using the BMD method in CAMHBT. High-level rifampicin resistance was defined with a MIC > 32 mg $L^{-1}$. All susceptibility testing was performed in triplicate.

**Whole-genome sequencing**

Genomic DNA was extracted from a single colony using a JANUS automated workstation (PerkinElmer) and Chemagic magnetic bead technology (PerkinElmer). Genomic DNA libraries were prepared using the Nextera XT kit according to manufacturer's instructions (Illumina, San Diego, CA, USA). Whole-genome sequencing was performed using Illumina NextSeq platform, generating 150 bp paired-end reads.

The short reads of isolates sequenced at MDU-PHL are available on the NCBI Sequence Read Archive [BioProjects PRJNA565795 (Controlling Superbugs), PRJNA433676 (2015 Snapshot) and PRJNA856406 (2018 Snapshot), and PRJNA856406 (historical *vanA* isolates)].

**Phylogenetic analysis**

De novo assemblies of the genomes were constructed using Spades[48] (v3.13). In silico MLST were determined using the program mlst with the efaecium database (https://github.com/tseemann/mlst). The 1000 Australian genomes as well as the 4,612 Australian and international VREfm were mapped to the reference *E. faecium* genome AUS0085 isolated from a human bacteraemia infection in Victoria, Australia (NCBI accession: CP006620)[47] using snippy (https://github.com/tseemann/snippy) (v4.4.5), applying a minfrac value of 10 and mincov value of 0.9. This reference was selected as it was a publicly available

556 complete genome collected locally and daptomycin-sensitive. A maximum likelihood
557 phylogenetic tree was inferred using IQ-TREE (v2.1.2) with a general time-reversible (GTR +
558 G4) substitution model, including invariable sites as a constant pattern and 1000 bootstrap
559 replicates. Recombination masking was not performed for species maximum likelihood trees
560 due to the small size of the resulting core alignment. All trees were mid-point rooted and
561 visualised in R (v4.0.3, https://www.r-project.org/) using phangorn[49] (v2.5.5), ape[50] (v5.4),
562 ggtree[51] (v2.3.4), and ggplot (v3.3.2).
563 The genome assemblies of all isolates were screened for acquired antimicrobial resistance
564 determinants using abriTAMR (https://github.com/MDU-PHL/abritamr).
565 **Genome-wide association study of daptomycin resistance**
566 A GWAS approach was applied to identify genetic variants of daptomycin resistance in *E.*
567 *faecium*. A genotype matrix of SNPs was constructed and used as input to homoplasyFinder[52]
568 (v0.0.0.9) to determine the consistency index at each locus and kept mutations that had an
569 index of ≤0.5 (indicating at least two independent acquisitions across the phylogeny). We then
570 ran GWAS using daptomycin resistance as a binary trait, where isolates were categorised as
571 resistant if their daptomycin MIC was ≥8 mg $L^{-1}$. To correct for population structure, we used
572 the factored spectrally transformed linear mixed models (FaST-LMM) implemented in
573 pyseer[53] (v.1.3.6), which computes a kinship matrix based on the core genome SNPs as a
574 random effect. The Bonferroni method was used to correct *P* values for multiple testing.
575 **Core genome MLST (cgMLST) and clustering**
576 cgMLST alleles for each isolate was defined using the public *E. faecium* cgMLST scheme[54] and
577 chewBBACA (v2.0.16), implemented locally in the COREugate pipeline (v2.0.4)
578 (https://github.com/kristyhoran/Coreugate). The pipeline determines the alleles of each core
579 gene for every isolate as defined by the specific pathogen scheme. The *E. faecium* cgMLST

scheme contains 1,423 genes. The number of allelic differences between each isolate within this core set of genes is then determined. The cgMLST clusters were determined using single linkage clustering and a pairwise allelic difference threshold of ≤250. This threshold was chosen since it maximised diversity within clusters, to improve temporal sampling depth, while still clustering based on maximum-likelihood tree structure.

**Phylodynamic analyses of the emergence of the S491F RpoB mutation in VREfm lineages**

To investigate the emergence of the S491F mutation in RpoB in three different lineages, as defined with cgMLST, we undertook further analysis on these clusters/lineages. From the species-level maximum-likelihood tree (Figure 3A), three lineages/clusters were identifiable by cgMLST due to their size (n>50) and presence of the S491F mutation. The three clusters were analysed independently, such that individual core-genome SNP alignments were generated, since this increased the length of the core alignment and number of sites considered. Snippy (https://github.com/tseemann/snippy) (v4.4.5) was used to generate the alignments for each cluster to the corresponding reference genome (AUSMDU00004024 for cluster 1, AUSMDU00004055 for cluster 2, and AUSMDU00004142 for cluster 3). Each core alignment used a within 'cluster reference' (complete genome of the same cluster) to maximise core-SNP alignment length. The reference for each cluster was chosen since they were a locally-collected, closed genome. Recombination was removed from the final alignment using Gubbins[55] (v.2.4.1) to ensure modelling was only informed by SNPs with tree-like evolution within the core genome. Maximum-likelihood trees for each of the three clusters were inferred from the core-SNP alignments [Cluster 1: (n=219 taxa) 329 SNPs; Cluster 2: (n=85 taxa) 541 SNPs; Cluster 3: (n=68 taxa) 764 SNPs] with IQ-tree (v2.1.2)[56] with a general time-reversible (GTR+$\Gamma$) substitution model, including invariable sites as a constant

603 pattern. Phylogenetic uncertainty was determined through 1000 nonparametric bootstrap
604 replicates.

605 To investigate temporal signal in the three clusters of VREfm genomes, we first used
606 TempEst[57] (v1.5). A root-to-tip regression analysis was performed on the root-to-tip branch
607 distances within the three, cluster maximum-likelihood phylogenies as a function of year of
608 collection, with the position of the root optimised according to the heuristic residual mean
609 squared method.

610 The frequency of the emergence of the *rpoB* mutation in VREfm was inferred using a
611 discrete trait model implemented in BEAST[58] (v1.10.4). Under this model the SNP alignments
612 are used to infer the evolutionary process (i.e. phylogenetic tree, time, and nucleotide
613 substitution model parameters) for the three clusters. The alignments all shared the HKY
614 substitution model with a gamma distribution for among-site rate variation, and a constant-
615 size coalescent population prior[28]. To avoid ascertainment bias due to using a SNP alignment,
616 the number of constant sites were taken into account for the likelihood calculations. The
617 molecular clock was a relaxed clock with an underlying lognormal distribution. The molecular
618 clock was calibrated using isolation dates for each genome by year of collection and the mean
619 clock rate is shared between all three alignments, but the model allows for the individual
620 alignments to have different standard deviations of the lognormal distribution and also
621 different branch rates. The mean molecular clock rate requires an explicit prior distribution,
622 for which we used a $\Gamma$ distribution and a 0.95 quantile range of $4.9 \times 10^{-6}$ and $1.1 \times 10^{-4}$
623 substitutions/site/year. This informative prior means that it acts as an additional source of
624 molecular clock calibration that can drive estimates, even in the absence of temporal signal.

625 The presence or absence of the S491F mutation in *rpoB* was used as a binary trait[59,60].
626 The trait model was shared between the three alignments, with the different Markov jumps

and rewards (ie changes of trait state and time spent in each state, respectively) recorded for each of the three alignments. The posterior distribution of model parameters was sampled using a Markov chain Monte Carlo of 100,000,000 iterations, sampling every 100,000 iterations. Two independent runs were run for the models. We assessed sufficient sampling from the stationary distributions by verifying the effective sample size of key parameters was around or above 200. The final maximum-clade credibility (MCC) trees were visualised in R (v4.0.3, https://www.r-project.org/) using ggtree[51] (v2.3.4). The Markov jumps for the *rpoB* trait for each alignment were visualised in R (v4.0.3, https://www.r-project.org/).

**Reconstruction of clinical mutations by allelic exchange**

The *liaR*$^{W73C}$, *liaS*$^{T120A}$, *rpoC*$^{T634K}$, *rpoB*$^{G482D}$, *rpoB*$^{H486Y}$, or *rpoB*$^{S491F}$ mutations were recombined into the chromosomal copy of each gene in ST796 VREfm (Ef_aus0233) by allelic exchange. The *liaR*$^{W73C}$ and *liaS*$^{T120A}$ mutations were first introduced individually, then together. The region encompassing each gene was amplified by SOE-PCR and recombined into pIMAY-Z[61] by the seamless ligation cloning extract (SLiCE)[62] method and transformed into *Escherichia coli* IM08B[61]. The construct was transformed into electrocompetent VREfm[62], with allelic exchange performed as described previously[63]. Allelic exchange was performed as described[63]. Reversion of *liaR*$^{W73C}$ and *liaS*$^{T120A}$, *rpoB*$^{G482D}$, *rpoB*$^{H486Y}$, or *rpoB*$^{S491F}$ mutations were completed using allelic exchange with a construct containing the respective wild-type allele. To delete the ABC transporter protein (EFAU085_02633), permease protein (EFAU02892), or mannitol dehydrogenase (EFAU02627) from the chromosome, deletion constructs were PCR-amplified from Ef_aus0233 genomic DNA and allelic exchange performed as described above. Genome sequencing and analysis of all mutants was conducted as described, with resulting reads mapped to the Ef_aus0233 reference genome and mutations identified using Snippy (https://github.com/tseemann/snippy) (v4.4.5).

**VREfm *in vivo* gastrointestinal colonisation experiments**

Female C57BL/6 mice at 6-8 weeks of age were purchased from WEHI and maintained in a specific-pathogen-free facility at the Peter Doherty Institute for Infection and Immunity. All animal handling and procedures were performed in a biosafety class 2 cabinet. Animal procedures were performed in compliance with the University of Melbourne guidelines and approved by the University's Animal Ethics Committee

The dose for each antibiotic was calculated using the FDA human conversion formula to ensure each mouse was given a human-equivalent dose[64]. To establish gastrointestinal colonisation of VREfm, mice were administered ceftriaxone (410 mg $kg^{-1}$ $day^{-1}$; AFT Pharmaceuticals) via subcutaneous injection once daily for 7 days, followed by an antibiotic wean period of 24 hours. Mice were then inoculated with $10^6$ VREfm in 100 µl PBS by oral gavage. Three days after VREfm inoculation, single-housed mice were administered either rifaximin (113 mg $kg^{-1}$ administered twice daily; Sigma Aldrich), rifampicin (123 mg $kg^{-1}$ administered once day; Sigma Aldrich), or vehicle (Corn oil with 10% DMSO) via oral gavage; or daptomycin (50 mg $kg^{-1}$ administered once daily; Cubicin) via subcutaneous injection [this results in similar exposure ($AUC_{0-24}$) to that observed in humans receiving 8 mg $kg^{-1}$ of intravenous daptomycin[65]]. The above antibiotic dosing protocol was followed for 7 days. Faecal samples were collected at specific time points throughout the experiment to determine VREfm gut colonisation and for downstream rifamycin and daptomycin resistance analysis. Faecal samples were resuspended in PBS to a normalised concentration (100 mg $ml^{-1}$). Serial dilutions were performed, and samples were plated onto Brilliance VRE agar (Oxiod) for VREfm CFU enumeration.

For rifamycin and daptomycin analysis, VREfm colonies (n=50 per mouse) from the Brilliance VRE agar plates were replica plated onto BHIA with and without rifampicin 20 mg $mL^{-1}$ to

675 determine the proportion of rifampicin-resistant VREfm in each mouse. All colonies (n=50 per
676 mouse) were then screened for daptomycin resistance using a daptomycin screen. Of which,
677 a single colony was resuspended in PBS, then diluted 1/100 into CAMHBT containing 50 mg $L^{-1}$ $Ca^{2+}$, and 1/100 in MH containing 50 mg $L^{-1}$ $Ca^{2+}$, and 8 mg $L^{-1}$ daptomycin. All suspected
679 daptomycin-resistant colonies were confirmed using a daptomycin BMD MIC as before.
680 To determine which mutations were present in the rifamycin-resistant isolates, a random
681 selection of 300 colonies, 150 from rifaximin treated mice and 150 from rifampicin treated
682 mice, were sampled for WGS as described above.

683 **Analysis of VREfm isolates from patients receiving rifaximin.**

684 To examine the potential association of rifaximin use in humans and the presence of
685 daptomycin-resistant VREfm strains, we analysed VREfm collected between 2018 and 2021
686 from a single hospital institution in Melbourne. These isolates underwent WGS and
687 daptomycin and rifampicin susceptibility testing as before. Isolates were stratified according
688 to whether the patient received rifaximin within 1 month of VREfm isolation or remained
689 rifaximin free prior to isolate collection. The majority (80%) of isolates were routine screening
690 samples. This included 50 VREfm isolates from patients receiving or previously receiving
691 rifaximin at time of isolation, which were randomly matched to 50 VREfm isolates from
692 patients not receiving rifaximin administration. All isolates were collected within the same
693 time frame. The VREfm isolates were visualised in a maximum-likelihood phylogenetic tree as
694 before, using a core-SNP alignment of 12,430 sites. Isolate MLST was defined with the mlst
695 tool and mutations in RpoB were determined using Snippy
696 (https://github.com/tseemann/snippy) (v4.4.5) as described.

697 **Data visualisation and statistics**

All figures were generated in R (v4.0.3, https://www.r-project.org/) using tidyverse (v.1.3.1), patchwork (v.1.1.1), and ggnewscale (v.0.4.5). Statistical analyses were performed using R (v4.0.3, https://www.r-project.org/) and GraphPad Prism (v9.3.1) software packages. Specific tests are given together with each result in the text.

**Ethics approval**

Ethical approval for analysis of patient data was received from the University of Melbourne Human Research Ethics Committee (study number 1954615.3).

**Competing Interests**

The authors declare no competing interests.

**Acknowledgements**

This work was supported by the National Health and Medical Research Council (NHMRC) of Australia (GNT1185213 and GNT1160745). BPH is supported by an NHMRC Investigator Grant (GNT1196103). JCK is supported by an NHMRC Early Career Fellowship (GNT1142613). AMT and NLS are supported by an Australian Government Research Training Program scholarship. The Controlling Superbugs study was supported by the Melbourne Genomics Health Alliance (funded by the State Government of Victoria, Department of Health and Human Services, and the 10 member organizations).

**Author Contributions**

GPC, BPH, and CLG conceived and planned the experiments. AMT, LL, IRM, DLI, SD, and GPC performed the planned experiments. JCK provided access to necessary patient metadata and clinical VREfm isolates that were used in the study. JYHL, NLS, TPS, and JCK provided critical clinical or bioinformatic insights for the study. AMT, CLG, and GPC co-wrote the manuscript with critical feedback and input from all authors.

**Corresponding Authors**

722 Correspondence to Glen Carter or Benjamin Howden.

723 **Data Availability**

724 The data presented in the study are deposited under Bioprojects PRJNA565795,

725 PRJNA433676, PRJNA856406, and PRJNA856406.

726

## References

1. Murray, C. J. *et al.* Global burden of bacterial antimicrobial resistance in 2019: a systematic analysis. *The Lancet* **399**, 629–655 (2022).
2. Bylicka-Szczepanowska, E. & Korzeniewski, K. Asymptomatic Malaria Infections in the Time of COVID-19 Pandemic: Experience from the Central African Republic. *Int. J. Environ. Res. Public. Health* **19**, 3544 (2022).
3. Global HIV & AIDS statistics — Fact sheet. https://www.unaids.org/en/resources/fact-sheet.
4. GBD 2019 Collaborators. Global mortality from dementia: Application of a new method and results from the Global Burden of Disease Study 2019. *Alzheimers Dement. N. Y. N* **7**, e12200 (2021).
5. Arias, C. A. & Murray, B. E. The rise of the *Enterococcus*: beyond vancomycin resistance. *Nat. Rev. Microbiol.* **10**, 266–278 (2012).
6. Top, J., Willems, R. & Bonten, M. Emergence of CC17 *Enterococcus faecium*: from commensal to hospital-adapted pathogen. *FEMS Immunol. Med. Microbiol.* **52**, 297–308 (2008).
7. Arthur, M. & Courvalin, P. Genetics and mechanisms of glycopeptide resistance in enterococci. *Antimicrob. Agents Chemother.* **37**, 1563–1571 (1993).
8. Tacconelli, E. *et al.* Discovery, research, and development of new antibiotics: the WHO priority list of antibiotic-resistant bacteria and tuberculosis. *Lancet Infect. Dis.* **18**, 318–327 (2018).
9. Montero, C. I., Stock, F. & Murray, P. R. Mechanisms of Resistance to Daptomycin in *Enterococcus faecium*. *Antimicrob. Agents Chemother.* (2008) doi:10.1128/AAC.00774-07.

10. Greene, M. H. *et al.* Risk Factors and Outcomes Associated With Acquisition of Daptomycin and Linezolid–Nonsusceptible Vancomycin-Resistant *Enterococcus*. *Open Forum Infect. Dis.* **5**, ofy185 (2018).

11. Egli, A. *et al.* Association of daptomycin use with resistance development in *Enterococcus faecium* bacteraemia—a 7-year individual and population-based analysis. *Clin. Microbiol. Infect.* **23**, 118.e1-118.e7 (2017).

12. Diaz, L. *et al.* Whole-Genome Analyses of *Enterococcus faecium* Isolates with Diverse Daptomycin MICs. *Antimicrob. Agents Chemother.* (2014).

13. Lellek, H. *et al.* Emergence of daptomycin non-susceptibility in colonizing vancomycin-resistant *Enterococcus faecium* isolates during daptomycin therapy. *Int. J. Med. Microbiol.* **305**, 902–909 (2015).

14. Kelesidis, T., Tewhey, R. & Humphries, R. M. Evolution of high-level daptomycin resistance in *Enterococcus faecium* during daptomycin therapy is associated with limited mutations in the bacterial genome. *J. Antimicrob. Chemother.* **68**, 1926–1928 (2013).

15. Werth, B. J. *et al.* Defining Daptomycin Resistance Prevention Exposures in Vancomycin-Resistant *Enterococcus faecium* and *E. faecalis*. *Antimicrob. Agents Chemother.* **58**, 5253–5261 (2014).

16. Turner, A. M., Lee, J. Y. H., Gorrie, C. L., Howden, B. P. & Carter, G. P. Genomic Insights Into Last-Line Antimicrobial Resistance in Multidrug-Resistant *Staphylococcus* and Vancomycin-Resistant *Enterococcus*. *Front. Microbiol.* **12**, (2021).

17. Li, L. *et al.* Daptomycin Resistance Occurs Predominantly in vanA-Type Vancomycin-Resistant *Enterococcus faecium* in Australasia and Is Associated With Heterogeneous and Novel Mutations. *Front. Microbiol.* **12**, 749935 (2021).

773 18. Bass, N. M. *et al.* Rifaximin Treatment in Hepatic Encephalopathy. *N. Engl. J. Med.*
774 **362**, 1071–1081 (2010).
775 19. Shayto, R. H., Abou Mrad, R. & Sharara, A. I. Use of rifaximin in gastrointestinal and
776 liver diseases. *World J. Gastroenterol.* **22**, 6638–6651 (2016).
777 20. Sherry, N. L. *et al.* Pilot study of a combined genomic and epidemiologic surveillance
778 program for hospital-acquired multidrug-resistant pathogens across multiple hospital
779 networks in Australia. *Infect. Control Hosp. Epidemiol.* **42**, 573–581 (2021).
780 21. Gorrie, C. L. *et al.* Key parameters for genomics-based real-time detection and
781 tracking of multidrug-resistant bacteria: a systematic analysis. *Lancet Microbe* **2**, e575–
782 e583 (2021).
783 22. Miller, W. R., Bayer, A. S. & Arias, C. A. Mechanism of Action and Resistance to
784 Daptomycin in *Staphylococcus aureus* and Enterococci. *Cold Spring Harb. Perspect. Med.*
785 **6**, a026997 (2016).
786 23. Prater, A. G. *et al.* Environment Shapes the Accessible Daptomycin Resistance
787 Mechanisms in *Enterococcus faecium. Antimicrob. Agents Chemother.* **63**, e00790-19.
788 24. Bæk, K. T. *et al.* Stepwise Decrease in Daptomycin Susceptibility in Clinical
789 *Staphylococcus aureus* Isolates Associated with an Initial Mutation in *rpoB* and a
790 Compensatory Inactivation of the clpX Gene. *Antimicrob. Agents Chemother.* (2015).
791 25. Cui, L. *et al.* An RpoB Mutation Confers Dual Heteroresistance to Daptomycin and
792 Vancomycin in *Staphylococcus aureus*. *Antimicrob. Agents Chemother.* (2010)
793 doi:10.1128/AAC.00437-10.
794 26. Goldstein, B. P. Resistance to rifampicin: a review. *J. Antibiot. (Tokyo)* **67**, 625–630
795 (2014).

796 27. Rios, R. *et al.* Genomic Epidemiology of Vancomycin-Resistant *Enterococcus faecium*
797 (VREfm) in Latin America: Revisiting The Global VRE Population Structure. *Sci. Rep.* **10**,
798 5636 (2020).
799 28. Duchêne, S. *et al.* Genome-scale rates of evolutionary change in bacteria. *Microb.*
800 *Genomics* **2**, e000094 (2016).
801 29. Lebreton, F. *et al.* Emergence of Epidemic Multidrug-Resistant *Enterococcus faecium*
802 from Animal and Commensal Strains. *mBio* **4**, e00534-13.
803 30. Raven, K. E. *et al.* A decade of genomic history for healthcare-associated
804 *Enterococcus faecium* in the United Kingdom and Ireland. *Genome Res.* **26**, 1388–1396
805 (2016).
806 31. Goel, A., Rahim, U., Nguyen, L. H., Stave, C. & Nguyen, M. H. Systematic review with
807 meta-analysis: rifaximin for the prophylaxis of spontaneous bacterial peritonitis. *Aliment.*
808 *Pharmacol. Ther.* **46**, 1029–1036 (2017).
809 32. Lee, R. A. *et al.* Daptomycin-Resistant *Enterococcus* Bacteremia Is Associated With
810 Prior Daptomycin Use and Increased Mortality After Liver Transplantation. *Open Forum*
811 *Infect. Dis.* **9**, ofab659 (2022).
812 33. Morley, V. J. *et al.* An adjunctive therapy administered with an antibiotic prevents
813 enrichment of antibiotic-resistant clones of a colonizing opportunistic pathogen. *eLife* **9**,
814 e58147 (2020).
815 34. Bender, J. K. *et al.* Update on prevalence and mechanisms of resistance to linezolid,
816 tigecycline and daptomycin in enterococci in Europe: Towards a common nomenclature.
817 *Drug Resist. Updat.* **40**, 25–39 (2018).

35. Tran, T. T. *et al.* Whole-Genome Analysis of a Daptomycin-Susceptible *Enterococcus faecium* Strain and Its Daptomycin-Resistant Variant Arising during Therapy. *Antimicrob. Agents Chemother.* **57**, 261–268 (2013).

36. Zaw, M. T., Emran, N. A. & Lin, Z. Mutations inside rifampicin-resistance determining region of *rpoB* gene associated with rifampicin-resistance in *Mycobacterium tuberculosis*. *J. Infect. Public Health* **11**, 605–610 (2018).

37. Lee, J. Y. H. *et al.* Global spread of three multidrug-resistant lineages of *Staphylococcus epidermidis*. *Nat. Microbiol.* **3**, 1175–1185 (2018).

38. Guérillot, R. *et al.* Convergent Evolution Driven by Rifampin Exacerbates the Global Burden of Drug-Resistant *Staphylococcus aureus*. *mSphere* **3**, e00550-17.

39. Albarillo, F. S., Medina, R. E., Joyce, C. S., Darji, H. & Santarossa, M. Daptomycin-resistant VRE infections: a descriptive analysis at a single academic centre. *Infect. Dis.* **53**, 393–395 (2021).

40. Teillant, A., Gandra, S., Barter, D., Morgan, D. J. & Laxminarayan, R. Potential burden of antibiotic resistance on surgery and cancer chemotherapy antibiotic prophylaxis in the USA: a literature review and modelling study. *Lancet Infect. Dis.* **15**, 1429–1437 (2015).

41. Berríos-Torres, S. I. *et al.* Activity of Commonly Used Antimicrobial Prophylaxis Regimens against Pathogens Causing Coronary Artery Bypass Graft and Arthroplasty Surgical Site Infections in the United States, 2006–2009. *Infect. Control Hosp. Epidemiol.* **35**, 231–239 (2014).

42. Dyar, O. J., Huttner, B., Schouten, J. & Pulcini, C. What is antimicrobial stewardship? *Clin. Microbiol. Infect.* **23**, 793–798 (2017).

840 43. Lee, R. S. *et al.* The changing landscape of vancomycin-resistant *Enterococcus*
841 *faecium* in Australia: a population-level genomic study. *J. Antimicrob. Chemother.* **73**,
842 3268–3278 (2018).
843 44. Snyder, E. E. *et al.* PATRIC: The VBI PathoSystems Resource Integration Center.
844 *Nucleic Acids Res.* **35**, D401–D406 (2007).
845 45. Wood, D. E., Lu, J. & Langmead, B. Improved metagenomic analysis with Kraken 2.
846 *Genome Biol.* **20**, 257 (2019).
847 46. Humphries, R. M. The New, New Daptomycin Breakpoint for *Enterococcus* spp. *J.*
848 *Clin. Microbiol.* **57**, e00600-19.
849 47. Lam, M. M. *et al.* Comparative analysis of the complete genome of an epidemic
850 hospital sequence type 203 clone of vancomycin-resistant *Enterococcus faecium*. *BMC*
851 *Genomics* **14**, 595 (2013).
852 48. Bankevich, A. *et al.* SPAdes: A New Genome Assembly Algorithm and Its Applications
853 to Single-Cell Sequencing. *J. Comput. Biol.* **19**, 455–477 (2012).
854 49. Schliep, K. P. phangorn: phylogenetic analysis in R. *Bioinformatics* **27**, 592–593
855 (2011).
856 50. Paradis, E. & Schliep, K. ape 5.0: an environment for modern phylogenetics and
857 evolutionary analyses in R. *Bioinformatics* **35**, 526–528 (2019).
858 51. Yu, G., Smith, D. K., Zhu, H., Guan, Y. & Lam, T. T.-Y. ggtree: an r package for
859 visualization and annotation of phylogenetic trees with their covariates and other
860 associated data. *Methods Ecol. Evol.* **8**, 28–36 (2017).
861 52. Crispell, J., Balaz, D. & Gordon, S. V. HomoplasyFinder: a simple tool to identify
862 homoplasies on a phylogeny. *Microb. Genomics* **5**, e000245 (2019).

863 53. Lees, J. A., Galardini, M., Bentley, S. D., Weiser, J. N. & Corander, J. pyseer: a
864 comprehensive tool for microbial pangenome-wide association studies. *Bioinformatics*
865 **34**, 4310–4312 (2018).
866 54. de Been, M. *et al.* Core Genome Multilocus Sequence Typing Scheme for High-
867 Resolution Typing of *Enterococcus faecium*. *J. Clin. Microbiol.* **53**, 3788–3797 (2015).
868 55. Croucher, N. J. *et al.* Rapid phylogenetic analysis of large samples of recombinant
869 bacterial whole genome sequences using Gubbins. *Nucleic Acids Res.* **43**, e15 (2015).
870 56. Nguyen, L.-T., Schmidt, H. A., von Haeseler, A. & Minh, B. Q. IQ-TREE: A Fast and
871 Effective Stochastic Algorithm for Estimating Maximum-Likelihood Phylogenies. *Mol. Biol.*
872 *Evol.* **32**, 268–274 (2015).
873 57. Rambaut, A., Lam, T. T., Max Carvalho, L. & Pybus, O. G. Exploring the temporal
874 structure of heterochronous sequences using TempEst (formerly Path-O-Gen). *Virus Evol.*
875 **2**, vew007 (2016).
876 58. Suchard, M. A. *et al.* Bayesian phylogenetic and phylodynamic data integration using
877 BEAST 1.10. *Virus Evol.* **4**, vey016 (2018).
878 59. Minin, V. N. & Suchard, M. A. Counting labeled transitions in continuous-time
879 Markov models of evolution. *J. Math. Biol.* **56**, 391–412 (2008).
880 60. Minin, V. N. & Suchard, M. A. Fast, accurate and simulation-free stochastic mapping.
881 *Philos. Trans. R. Soc. B Biol. Sci.* **363**, 3985–3995 (2008).
882 61. Monk, I. R., Tree, J. J., Howden, B. P., Stinear, T. P. & Foster, T. J. Complete Bypass of
883 Restriction Systems for Major *Staphylococcus aureus* Lineages. *mBio* **6**, e00308-15.
884 62. Zhang, Y., Werling, U. & Edelmann, W. Seamless Ligation Cloning Extract (SLiCE)
885 Cloning Method. in *DNA Cloning and Assembly Methods* (eds. Valla, S. & Lale, R.) 235–244
886 (Humana Press, 2014). doi:10.1007/978-1-62703-764-8_16.

887 63. Pidot, S. J. *et al.* Increasing tolerance of hospital *Enterococcus faecium* to handwash
888 alcohols. *Sci. Transl. Med.* **10**, eaar6115 (2018).
889 64. Nair, A. B. & Jacob, S. A simple practice guide for dose conversion between animals
890 and human. *J. Basic Clin. Pharm.* **7**, 27–31 (2016).
891 65. Heine, H. S., Bassett, J., Miller, L., Purcell, B. K. & Byrne, W. R. Efficacy of Daptomycin
892 against *Bacillus anthracis* in a Murine Model of Anthrax Spore Inhalation. *Antimicrob.*
893 *Agents Chemother.* **54**, 4471–4473 (2010).
894
895

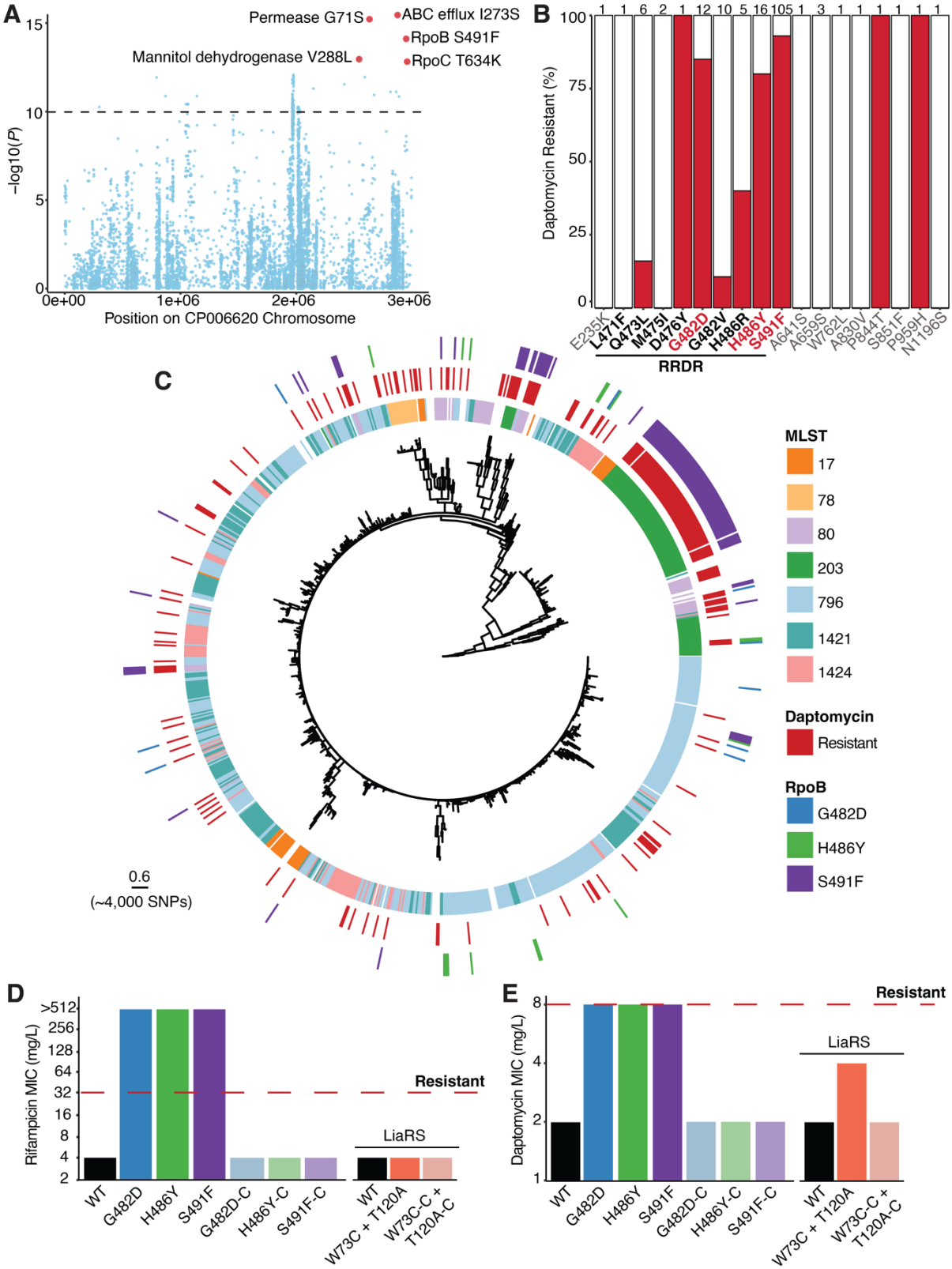


896

**Figure 1. A.** Manhattan plot of 10,530 variants, displayed by position on the reference genome and significance association with daptomycin resistance (univariate analysis using a linear mixed model). The dashed line shows the Bonferroni-corrected significance threshold. **B.** Percentage of daptomycin-resistant strains for each mutation within RpoB. The mutations within the rifampicin resistance determining region (RRDR) are shown in bold. Mutations coloured in red were associated with daptomycin resistance. The total number of strains containing each mutation is shown above each bar. **C.** Maximum-likelihood core-SNP-based phylogeny of clinical VREfm (n=1000) inferred from 6,574 SNPs, demonstrating the presence of RpoB mutations in daptomycin-resistant isolates. Overlaid are the results of *in silico* multi-locus sequence type (MLST), daptomycin phenotypic testing, and mutations associated with daptomycin resistance in RpoB. In the first circle, ST is not shown for uncommon STs (n≤5). The scale bar indicates number of nucleotide substitutions per site (top), with an approximation of SNP distance (in parentheses). **D.** Rifampicin susceptibility testing results for the WT, isogenic *rpoB* and *liaRS* isogenic mutants and complement strains (designated with -C) (n=3). **E.** Daptomycin susceptibility testing results for the WT, *rpoB* and *liaRS* isogenic mutants and complement strains (designated with -C) (n=3). The median MIC for each strain is shown.

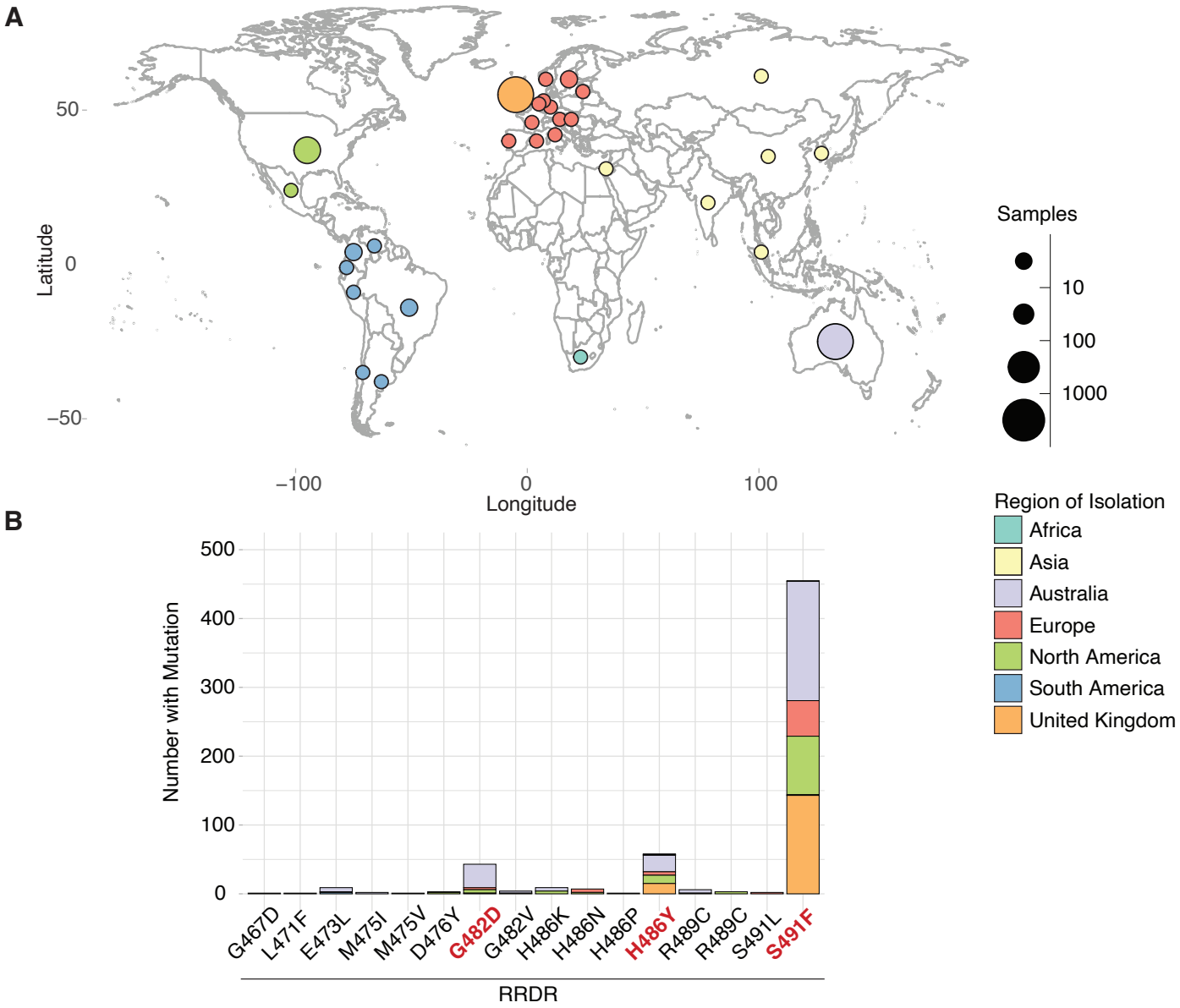
A
50
0
−50
Latitude
−100
0
100
Longitude
Samples
10
100
1000
B
Number with Mutation
500
400
300
200
100
0
G467D
L471F
E473L
M475I
M475V
D476Y
G482D
G482V
H486K
H486N
H486P
H486Y
R489C
R489C
S491L
S491F
RRDR
Region of Isolation
Africa
Asia
Australia
Europe
North America
South America
United Kingdom

915 **Figure 2. A.** Map of 4,476 VREfm genomes included in this study. Circle size corresponds to
916 total number of genomes (binned into categories), and colour corresponds to region of
917 isolation. Country coordinates used are the country centroid position. Map was generated in
918 R using ggplot2. **B.** The frequency of various RpoB mutations within the rifampicin resistance
919 determining region (RRDR) in 4,476 VREfm genomes, sampled from 43 MLSTs. Bars are
920 coloured by the number of isolates from each region of isolation containing the mutation. The
921 identified daptomycin resistance associated mutations are coloured in red.

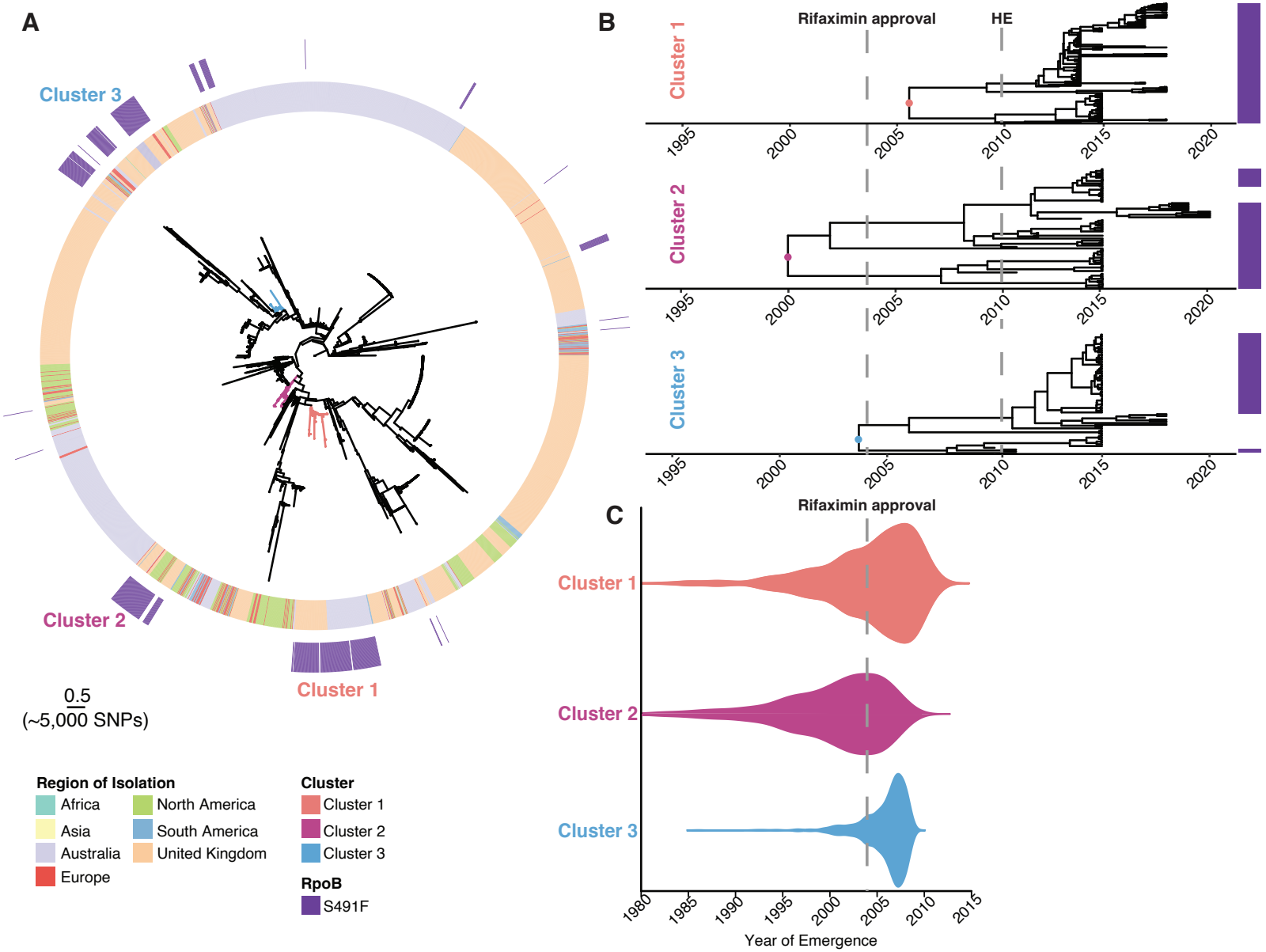
A
Cluster 3
Cluster 2
Cluster 1
0.5
(~5,000 SNPs)
Region of Isolation
Africa
Asia
Australia
Europe
North America
South America
United Kingdom
Cluster
Cluster 1
Cluster 2
Cluster 3
RpoB
S491F
B
Rifaximin approval
HE
Cluster 1
Cluster 2
Cluster 3
1995
2000
2005
2010
2015
2020
C
Rifaximin approval
Cluster 1
Cluster 2
Cluster 3
1980
1985
1990
1995
2000
2005
2010
2015
Year of Emergence

**Figure 3. A.** Maximum-likelihood, core-SNP-based phylogeny for 4,476 VREfm inferred from 9,277 core-genome SNPs, demonstrating the presence of the S491F RpoB mutation in international VREfm. Overlaid is the region of isolation for each strain and the presence of the S491F mutation. The coloured branches indicate the three VREfm clusters identified with cgMLST used as input for Bayesian evolutionary analyses. The scale bar indicates number of nucleotide substitutions per site (top), with an approximation of SNP distance (in parentheses). **B.** Bayesian phylodynamic analyses showing the maximum-clade credibility (MCC) trees of the three VREfm clusters with the timing of emergence for each lineage. Cluster 1 (n=219) was inferred from a core alignment of 1,869,554 bp containing 329 SNP sites; Cluster 2 (n=85) was inferred from an alignment of 1,524,024 bp containing 541 SNP sites; and Cluster 3 (n=68) was inferred from an alignment of 1,860,780 bp containing 764 SNP sites. The time in years is given on the *x* axis. The presence of the S491F RpoB trait for each isolate is shown in purple. Overlaid onto the MCC trees is the first instance of FDA approval for rifaximin (2004) and for hepatic encephalopathy (HE) (2010). **C.** Violin plots for the most recent common ancestor (MCRA) for each cluster, representing when the RpoB S491F mutation first emerged, with 95% HPD intervals. Overlaid onto violin plots is the FDA approval date for rifaximin (2004).

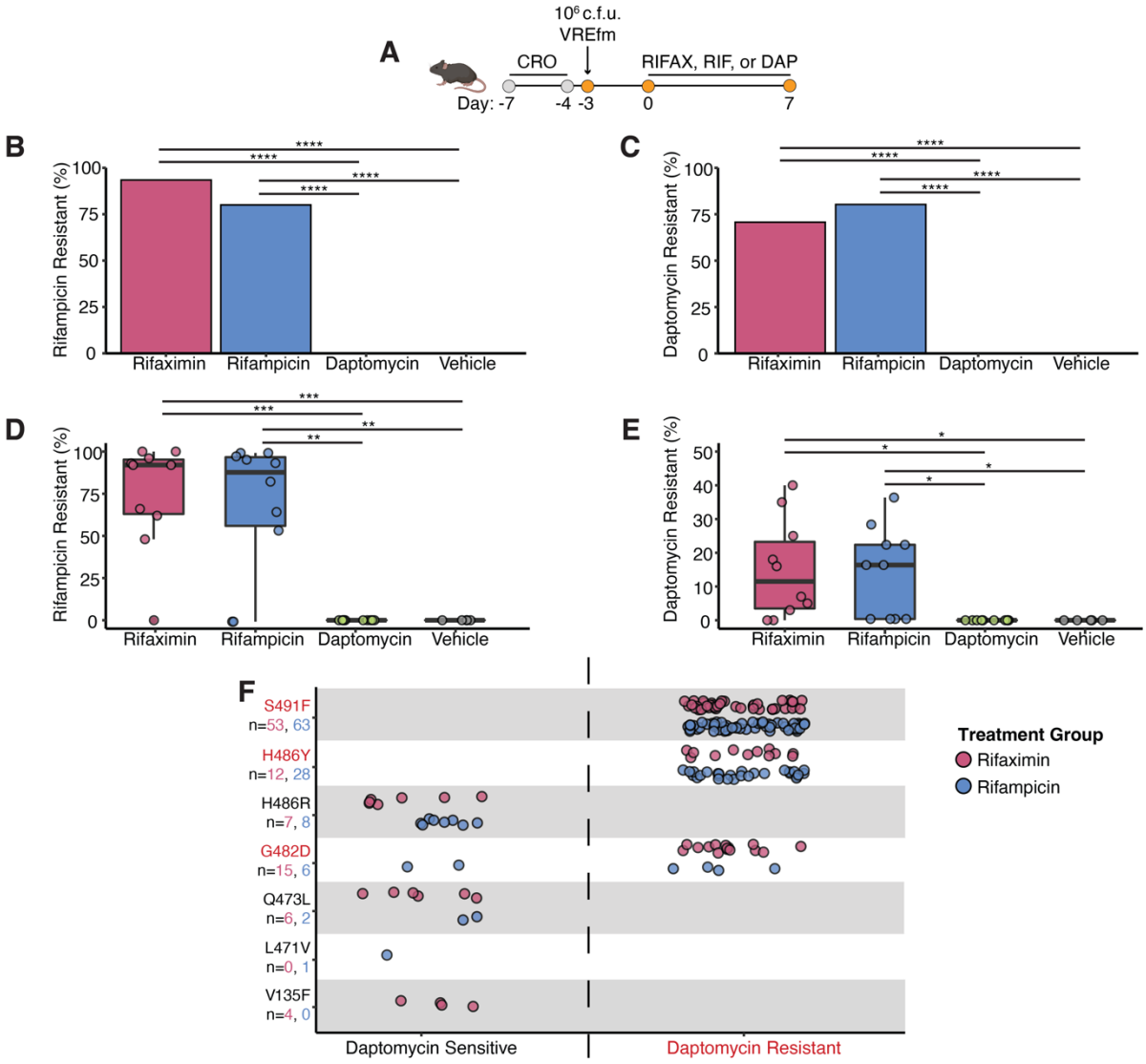


940

941 **Figure 4. A.** Timeline of the mouse experiment. VREfm-colonised mice (n=5 for vehicle, n=10
942 for rifampicin, n=10 for rifaximin, n=10 for daptomycin) received a human-equivalent dose of
943 vehicle, rifampicin, or rifaximin (twice per day for rifaximin) for 7 days by oral gavage or
944 subcutaneous injection with daptomycin for 7 days. CRO=ceftriaxone; DAP=daptomycin;
945 RIFAX=rifaximin; RIF=rifampicin. Figure to scale. **B.** Percentage of total mice with rifampicin-
946 resistant VREfm strains **C.** or daptomycin-resistant VREfm strains after 7 days of antibiotic
947 treatment. **D.** Percentage of VREfm from each mouse (n=50 colonies per mouse) that were
948 resistant to rifampicin **E.** or daptomycin after 7 days of antibiotic treatment. Points represent
949 an individual mouse. Percentage was calculated from rifampicin or daptomycin MIC values
950 (either resistant or susceptible) from 50 VREfm colonies isolated from each mouse. Boxes
951 represent the median and interquartile range for each group. **F.** Overview of the RpoB
952 mutations identified in the rifampicin-resistant colonies. Each point represents a single
953 colony. Isolates are separated by each RpoB mutation and grouped into either daptomycin-
954 susceptible or daptomycin-resistant. The RpoB mutations coloured in red had an association
955 with daptomycin resistance. n values represent the number of isolates containing each
956 mutation for rifaximin and rifampicin, respectively. *$P$ < 0.05, **$P$ < 0.01, ***$P$ < 0.001,
957 ****$P$<0.0001; unpaired *t*-test (vehicle versus rifampicin or vehicle versus rifaximin and
958 rifampicin verses daptomycin or rifaximin verses daptomycin).

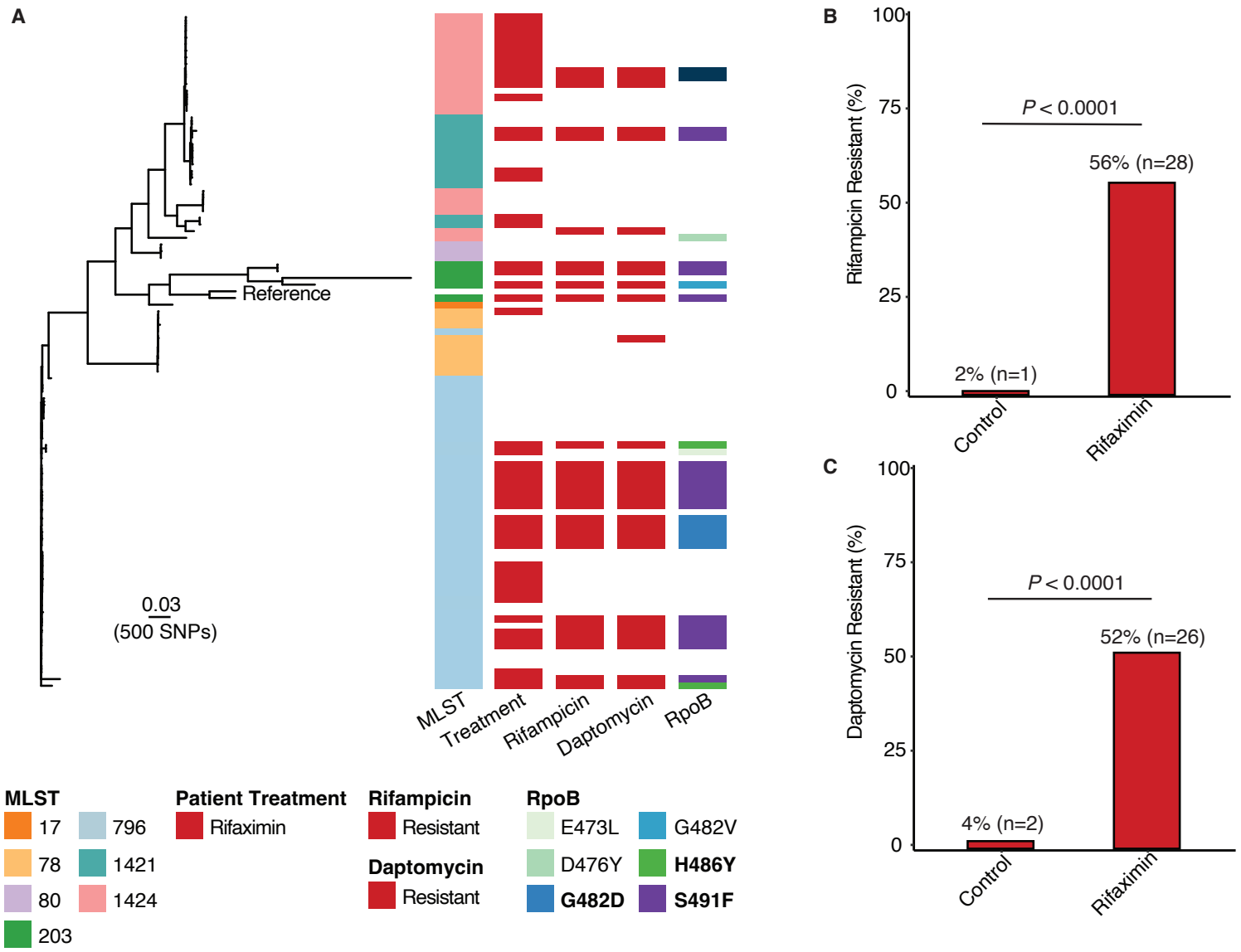
A
Reference
0.03
(500 SNPs)
MLST
Treatment
Rifampicin
Daptomycin
RpoB
MLST
17
78
80
203
796
1421
1424
Patient Treatment
Rifaximin
Rifampicin
Resistant
Daptomycin
Resistant
RpoB
E473L
D476Y
G482D
G482V
H486Y
S491F
B
Rifampicin Resistant (%)
100
75
50
25
0
P < 0.0001
56% (n=28)
2% (n=1)
Control
Rifaximin
C
Daptomycin Resistant (%)
100
75
50
25
0
P < 0.0001
52% (n=26)
4% (n=2)
Control
Rifaximin

960 **Figure 5. A.** Maximum-likelihood core-SNP-based phylogeny of clinical VREfm (n=100)
961 inferred from 12,430 SNPs. Overlaid is the results of *in silico* MLST, rifaximin treatment group,
962 rifampicin phenotypic testing, daptomycin phenotypic testing, and mutations in RpoB.
963 Mutations associated with daptomycin resistance are bolded. The scale bar indicates number
964 of nucleotide substitutions per site (top), with an approximation of SNP distance (in
965 parentheses). **B.** Rifampicin susceptibility data for clinical VREfm (n=50 per group). Red bars
966 represent percent of rifampicin-resistant isolates. A Fisher's exact test comparing the
967 percentage of rifampicin resistance in the control versus rifaximin, $P < 0.0001$. **C.** Daptomycin
968 susceptibility data for clinical VREfm (n=50 per group). Red bars represent percent of
969 daptomycin-resistant isolates. A Fisher's exact test comparing the percentage of daptomycin
970 resistance in the control versus rifaximin, $P < 0.0001$.